NASA TECHNICAL MEMORANDUM

NASA TM X-52805

NASA TM X-52805

EXPERIMENTAL CONFIRMATION OF CYCLIC THERMAL JOINT CONDUCTANCE

by Daniel J. McKinzie, Jr.
Lewis Research Center
Cleveland, Ohio

TECHNICAL PAPER proposed for presentation at
Fifth Thermophysics Conference sponsored by the
American Institute of Aeronautics and Astronautics
Los Angeles, California, June 29-July 1, 1970

EXPERIMENTAL CONFIRMATION OF CYCLIC THERMAL JOINT CONDUCTANCE

by Daniel J. McKinzie, Jr.

Lewis Research Center
Cleveland, Ohio

TECHNICAL PAPER proposed for presentation at

Fifth Thermophysics Conference sponsored by the
American Institute of Aeronautics and Astronautics
Los Angeles, California, June 29-July 1, 1970

NATIONAL AERONAUTICS AND SPACE ADMINISTRATION

EXPERIMENTAL CONFIRMATION OF CYCLIC THERMAL JOINT CONDUCTANCE

Daniel J. McKinzie, Jr.

Lewis Research Center
National Aeronautics and Space Administration
Cleveland, Ohio

E-5293

Abstract

Experimental heat transfer data obtained from a tungsten-tungsten and an Armco Iron-Armco Iron specimen have confirmed the Bowden and Tabor model of elasto-plastic events which occur during the cyclic engagement of surfaces in the lightly loaded range (4.45×10^5 to 3.45×10^6 N/m^2 or 64.5 to 500 psi). The specimens consisted of cylinders having a diameter of 2.54 cm. Their surfaces of contact were outgassed before the tests were conducted and each was run in a high vacuum environment of approximately 10^{-6} torr. The contact surfaces of the tungsten specimen were nominally flat and had an arithmetic average roughness height of approximately 7.0×10^{-7} m. The Armco iron specimen's surfaces had an arithmetic average roughness height of approximately 0.25×10^{-7} m and approximated spherical caps having a one-half wavelength. The contacting surfaces of both specimens were extensively surveyed in roughness height, waviness, and profile before the tests were performed. A recently published simplified approximate theory for calculating the coefficient of thermal contact conductance of plastically deforming nominally flat surfaces was applied to the tungsten specimen and was found to agree well with the data. This theory does not require the use of a computer program or the calculation of any abstract quantities. It does, however, require the use of a surface analyzer and microhardness tester. Clausing and Chao's macroscopic elastic theory of deformation was applied to the Armco Iron specimen and the agreement was found to be good.

Introduction

The design of space vehicle's internal and external structure and instrumentation will require varied regulated thermal conditioning[1], the extent of which has never been attempted until now. Because of the frequent use of lightly loaded (4.45×10^5 to 3.45×10^6 N/m^2 or 64.5 to 500 psi) friction-pressure dependent fasteners in vehicular design,[2] the ability to theoretically predict heating rates across their contact interfaces is important.

In 1950 Bowden and Tabor[3] presented a mechanical description of the mechanism of metallic contact between surface asperities without heat transfer effects. It included the loading, work hardening, and unloading of such asperities. During these events the elastic and plastic (reversible and irreversible, respectively) deformation of surface asperities occurs.

Fried,[4] Clausing and Chao,[5] and others present data demonstrating the variation of the coefficient of thermal contact conductance with pressure in a vacuum environment for one or several complete loading cycles, but they do not demonstrate theoretical agreement for the complete cycle. Frequently investigators label what they assume to be inconsistances in cyclic test results as exhibiting hysteresis effects. Thus the explicit cause of these effects is not given, though perhaps in some cases it is suggested.

The purposes of the present work are as follows:

(1) To describe the Bowden and Tabor model of metallic asperity contact.

(2) To present test data from both a tungsten-tungsten cylindrical specimen and an Armco iron-Armco iron cylindrical specimen. These data demonstrate the cyclic variation of the coefficient of thermal contact conductance with the apparent joint contact pressure in the lightly loaded range.

(3) To present some of the surface analyzer traces of the Armco iron specimen's interface surfaces of contact which were extensively surveyed to determine the variation of their surface roughness heights, waviness, and profile before the tests were conducted.

(4) To compare the complete cycle of each specimen's test data with the mechanism of the contact phenomena described in the Bowden and Tabor model.

(5) To make a comparison of the specimens' test data where applicable with the macroscopic elastic deformation theoretical analysis of Clausing and Chao[5] and Clausing,[6] and the recently published simplified plastic deformation theory of Ref. 7.

Theoretical Considerations

Bowden and Tabor Description of the Contact Phenomena

Bowden and Tabor in Ref. 3 describe in detail the mechanical aspects of the loading and unloading of a single work hardened surface asperity through which no heat transfer takes place. The tip of the asperity is assumed to be smooth and spherical in shape. Further, it is assumed to rest on a softer metal, and, in the region of contact, the surface of the softer metal is considered to be a plane. Fig. 1 shows what happens as the load on the asperity is increased. As the load on a single work hardened asperity is increased, an initial elastic deformation of the area of contact occurs; this is predicted by Hertz's classical equations. The planar projection of the area of contact A'_c varies with the load W' according to

$$A'_c \propto (W')^{2/3} \tag{1}$$

At some larger load the onset of plastic deformation takes place, and the area of contact varies with load according to

$$A_c' \propto W' \tag{2}$$

If the asperity is then unloaded from some higher load W_0' and area of contact $A_{c,0}'$, the variation of contact area with load is indicated by the dashed curve labeled reversible elastic deformation and is expressed by Eq. (1). If the load is removed, an offset in the area of contact $A_{c,1}'$ due to plastic deformation will persist. This description does not apply to the limiting case of a specimen whose interface of contact is composed of two very flat surfaces or whose surfaces of contact deform plastically under load to equivalent flat plates.

Clausing and Chao Macroscopic Theory

In Ref. 5 Clausing and Chao present their macroscopic theory of constrictive resistance. The constrictive resistance is defined as the reciprocal of the product of the apparent contact area, A, and the coefficient of thermal contact conductance, h. The apparent contact area is equal to the total cross-sectional area of their cylindrical model. Their model is shown in Fig. 2 which is similar to one appearing in Ref. 5. The theory considers the contact region between two cylinders of length L and identical radius b placed end to end. The ends of the cylinders in the contact plane have radii of curvature r_1 and r_2 (top and bottom, respectively) as shown in Fig. 2. A single large, macroscopic, circular contact area of radius a is assumed to be concentric with that of the apparent contact area. Thus the non-contact region is an annulus whose inside and outside radii are a and b, respectively. Microscopic contact areas are located inside the macroscopic contact; they are assumed circular, of the same radius, and uniformly distributed over the single macroscopic spot. Because of the annular non-contact region, the surfaces cannot be characterized as being nominally flat. Further, as a result of making numerical calculations examining the influence of the heat flux distribution on the local temperature over the circular contact areas Clausing and Chao arrived at a significant conclusion for their model. They concluded that macroscopic constrictive resistance, based on the macroscopic area of contact, is, within limits, independent of the magnitude and radial distribution of the microscopic constrictive resistance which is a function of the microscopic areas of contact. This, of course, only applies for the model considered. Thus, the Clausing and Chao macroscopic theory can be used to predict the coefficient of thermal contact conductance between wavy surfaces with the spherical contour of Fig. 2 representing one-half wave length. The form of the solution taken from Ref. 6 and used in this paper is

$$\frac{hb}{k} = \frac{1}{2\left[10^{f(x_c)}\right]} \tag{3}$$

where the limits of its application are

$$\left\{ \begin{array}{c} L/b > 0.8 \\ 0.16 < x_c < 0.84 \end{array} \right\}$$

L is defined as the length of the specimen's upper or lower piece, b is its radius and

$$f(x_c) = (1.39839 - 7.44698\, x_c + 19.9303\, x_c^2 - 38.5897\, x_c^3 + 38.6553\, x_c^4 - 16.6247\, x_c^5)$$

where x_c is the constriction ratio or equivalently the square root of the area ratio of contact. From Ref. 5 for two spherical surfaces in contact

$$x_c = 1.285\left[\frac{3W}{4b^3}\left(\frac{1-\nu_1^2}{E_1}+\frac{1-\nu_2^2}{E_2}\right)\left(\frac{1}{r_1}+\frac{1}{r_2}\right)^{-1}\right]^{1/3} \tag{4}$$

where ν_1 and ν_2 are Poisson's ratio which for most metals one may assume $\nu_1^2 = \nu_2^2 = 0.1$, E_1 and E_2 are the moduli of elasticity, W is the applied load, and r_1 and r_2 are the radii of curvature of the spherical surfaces.

Simplified Method of Reference 7

The simplified method of Ref. 7 gave an approximate parametric relation for the coefficient of thermal contact conductance. It was derived for two rough, nominally flat, outgassed surfaces in contact in a high vacuum. The asperities on the surfaces were assumed to be undergoing plastic deformation. The analysis was based on the steady-state Fourier one-dimensional heat conduction law. It was applied to the so-called "button" model of contact (described later in this section). Also included was a derivation of a parametric relation between the coefficient of thermal contact conductance and the contact pressure for the unloading of two surfaces.

Fig. 3 (modified from ref. 7) is a view of the assumed contact interface showing a contact region labeled the effective zone of the thermal disturbance. The length of this zone (defined later in this paper) is assumed to be a function of the sum of the largest asperity heights from each of the surfaces. This length is used as the best measurable dimension approximating the physical length of the zone of the thermal disturbance. Because this length only approximates the actual length over which the thermal discontinuity at the interface takes place, it is referred to as the effective zone of the thermal disturbance.

The following assumptions apply to the theoretical model which is used to approximate a test specimen.

(1) The specimen's contacting surface asperities are each replaced by the "button" model of contact.

(2) Each button contact is thermally insulated from its neighbor.

(3) The number of button contacts is uniformly distributed over the interface of contact.

(4) The axial temperature distribution in each cylinder of a button contact is the same as every other one. Thus, their circular areas of contact may be summed. The resulting single area of contact is shown in Fig. 4 (modified from ref. 7) and is referred to as "the button contact."

(5) The face of the button contact is in a state of plastic deformation with increasing load.

(6) No thermal gradient exists in the radial direction of the cylindrical button contact.

(7) The axial temperature gradient is constant and remains steady in time throughout the cylindrical volume of the button contact and the remainder of the model.

(8) The length of the effective zone of the thermal disturbance is very small and is equal to the sum of the lengths of the button contacts of the upper and lower portions of the model. It is therefore assumed that only within the effective zone of the thermal disturbance does the thermal discontinuity at the interface exist and that the thermal gradient in this zone is constant and steady in time.

(9) The interface of contact between the button contacts is assumed to be located at a point one-half the axial length of δ (see fig. 5). This assumption is made though the lengths of the button contacts δ_1 and δ_2 shown in Fig. 4 are not necessarily equal. This relocation does not introduce an error into the theoretical analysis because the length of δ is assumed to be very small. Thus the change in the mean temperature of the interface of contact is negligible (see fig. 5).

When these assumptions are applied to the model, the axial temperature distribution in the vicinity of the interface is as shown in Fig. 5. The basic steady-state one-dimensional Fourier heat conduction law written for the effective zone of the thermal disturbance δ (figs. 4 and 5) is given by

$$\frac{\dot{Q}}{A_c} = -k\frac{dt}{dx} \tag{5}$$

where A_c is the sum of the individual cross-sectional areas of the idealized individual "button" contacts, and k is the coefficient of thermal conductivity. This coefficient is evaluated at a temperature equal to $(t_{i,1} + t_{i,2})/2$ (see fig. 5), and dt/dx is the axial temperature gradient across the disturbance zone δ.

If Eq. (5) is applied to the effective zone of the thermal disturbance the heat-transfer rate per unit area at the interface of contact may be approximated by

$$\frac{\dot{Q}}{A_c} = -\frac{k(t_2 - t_1)}{\delta} \tag{6}$$

The coefficient of thermal contact conductance h is defined in the equation

$$\frac{\dot{Q}}{A} = -h\Delta t \tag{7}$$

where A is the cross-sectional area of the specimen. If the temperature gradients in the specimen outside the effective zone of the thermal disturbance are linearly extrapolated to the interface $x = 0$, as shown in Fig. 5, then Δt at the interface is given by

$$\Delta t = t_{i,2} - t_{i,1} \tag{8}$$

Substituting Eq. (8) into Eq. (7) gives

$$\frac{\dot{Q}}{A} = -h(t_{i,2} - t_{i,1}) \tag{9}$$

Equating the heat-transfer rate $\dot{Q}$ across the interface, Eqs. (6) and (9), yields

$$kA_c\frac{(t_2 - t_1)}{\delta} = Ah(t_{i,2} - t_{i,1}) \tag{10}$$

Since δ is very small, it is reasonable to assume that

$$t_2 - t_1 \cong t_{i,2} - t_{i,1} \tag{11}$$

Eq. (10) thus reduces to

$$\frac{h\delta}{k} = \frac{A_c}{A} \tag{12}$$

From plastic theory for nominally flat surfaces in contact (ref. 8),

$$\frac{A_c}{A} = \frac{P}{I} \tag{13}$$

where P is the pressure acting over the apparent surface in contact A, and I is the average of the random microhardness values of the softer of the two interface surfaces. Substituting Eq. (13) into Eq. (12) results in the desired equation

$$h\frac{\delta}{k} = \frac{P}{I} \tag{14}$$

Unloading the Contacting Surfaces

For the unloading of the contacting surfaces from a plastically deforming pressure at a constant mean interface temperature, Eq. (1) can be applied to the summation of the individual contact areas. If a maximum load W_0 is applied, the area of contact $A_{c,0}$ has the same magnitude for the elastic and plastic regime. Using Eqs. (1) and (12) at load W_0 yields

$$\frac{h_0\delta}{k} \propto \frac{W_0^{2/3}}{A} \tag{15}$$

or in terms of the pressure P_0

$$\frac{h_0\delta}{k} \propto \frac{P_0^{2/3}}{A^{1/3}} \tag{16}$$

In the elastic regime at a constant interface temperature assume δ/k is equal to a constant, C. If now the interface is unloaded from P_0 to P_1

$$\frac{(hC)_0}{(hC)_1} = \frac{\dfrac{P_0^{2/3}}{A^{1/3}}}{\dfrac{P_1^{2/3}}{A^{1/3}}} \tag{17}$$

where $A_0 = A_1$ and $C_0 = C_1$. Eq. (17) thus reduces to

$$h_1 = \left(\frac{P_1}{P_0}\right)^{2/3} h_0 \tag{18}$$

or substituting Eq. (14) into Eq. (18) yields

$$h_1 = P_1^{2/3} P_0^{1/3} \frac{k}{\delta I_0} \tag{19}$$

Thus Eq. (19) provides a method for calculating the coefficient of thermal contact conductance for any point below the upper limit of P_0 and h_0. This is true if the mean interface temperature of the contacting surfaces and heights of the plastically deformed asperities remain constant or very nearly constant during the unloading processes. It does not apply to flat surfaces or those surfaces which plastically deform under load to flat surfaces.

Experimental Apparatus and Procedure

Tungsten Specimen Test Apparatus

The tungsten-tungsten specimen was tested in the facility shown in Fig. 6. The test was performed in a bell jar containing an induction heating coil and a column composed of the test specimen, a OFHC copper heat meter, and water cooled heat sink as shown in Fig. 6. A pneumatic loading cylinder was located on top of the bell jar and was used to vary the pressure at the contact interface of the test specimen. Electric currents were induced in the extreme upper portion of the test specimen. The heat generated by these currents was transferred across the test interface, through the heat meter, and finally to the water cooled heat sink. The test specimen and heat meter were instrumented with thermocouples located as shown in Fig. 6. The thermocouples were read out on a potentiometer. The bell jar operates in the 10^{-6} torr pressure range.

Heating coil. - Because an induction coil was used to heat the specimen some further discussion of its effect on the specimen is needed. Although the magnetic field produced by the coil had a maximum value during the entire test of approximately 3.06×10^{-5} tesla at the center of the coil's axis, the effect on the tungsten-tungsten specimen was negligible since tungsten is nonferrous and has a magnetic permeability of approximately 1.000068 times that of free space. The effect of the induction coil's magnetic field on the thermocouples was also negligible. This was because the leads from each of the thermocouples were twisted for some distance away from the zone of the coil and specimen and they had no loops in them.

The use of the magnetic induction coil as the heat source created the possibility of electric current flowing through a circuit composed of the test column and the bell jar. The flow of current through this circuit was prevented by isolating the heat sink and its water cooling lines from the base plate and instrument ring of the bell jar.

Specimen. - The tungsten test specimen was metallurgically prepared from high purity pressed and sintered powder. The cylindrical specimen was 2.54 cm in diameter, its upper portion was 25.4 cm long so that it passed completely through the induction coil, and its lower portion was 2.54 cm long.

Surface finish. - The lay of the specimens interface surfaces was produced by grinding. The average value of the maximum roughness height across the lay of the upper and lower surfaces was 5.35 and 5.51 μm, respectively. The definition of this length and its measurement is included later in this section. The arithmetic average roughness height of the upper and lower surfaces was 0.538 and 0.943 μm, respectively. This length is defined in Ref. 9. The test was performed with the lay of the top and bottom surfaces approximately parallel. It was found that the maximum waviness height of the half wave length surfaces was less than the average value of their maximum roughness heights. This fact supports the assumption that the specimen's surfaces were nominally flat.

Thermometry. - Type 30 gage, special error limits, chromel-alumel thermocouple wire twisted at its ends was selected. These thermocouples have an accuracy of ± 1.1 K as guaranteed by the manufacturer in the temperature range of their use here. They were peened into holes 0.32 cm deep in the surface of the cylindrical specimens. As shown in Fig. 6, six thermocouples were located on the upper and five on the lower portion of the specimen. Also three sets of two approximately 180 degrees apart were located on the OFHC copper heat meter. The data from the thermocouples located at 0.32 cm on either side of the interface were not included in the data reduction. This was done because they were believed affected by the thermal discontinuity at the interface.

For a more detailed account of the tungsten specimen and the apparatus used to test it, see Ref. 7.

Armco Iron Specimen Test Apparatus

The Armco iron specimen was tested in the same facility as that used to test the tungsten specimen with the following exceptions. The magnetic induction heating coil was removed and replaced with a tungsten resistance heated cylindrical heat source. The length of the upper portion of the Armco iron specimen was appropriately made shorter to allow for the heater to fit into the test column above it. The OFHC heat meter was removed and replaced with an elongated lower portion of the Armco iron specimen which was especially instrumented and calibrated to replace the heat meter. With these revisions and the addition of a supporting structure for the new heat source, the flow of heat through the

test column, across the contacting surfaces, and then to the water cooled heat sink remained the same as described for the tungsten specimen.

Specimen. - The Armco iron cylindrical specimen was 2.54 cm in diameter. Its upper portion was 6.97 cm long and its lower portion was 12.7 cm long.

Surface finish. - The specimen's contacting interface surfaces were produced by lapping and had no lay. Fig. 7 shows several typical traces of the Armco iron specimen's top surface of contact. The average values of the maximum roughness heights determined from profile traces of the upper and lower surfaces of contact were 0.64×10^{-6} and 0.97×10^{-6} m, respectively; their arithmatic average roughness heights were 0.0381×10^{-6} m and 0.102×10^{-6} m, respectively. Each surface was found to approximate a section of a spherical cap having a one-half wave length. The average crest to trough height was approximately 1.52×10^{-6} m for the upper surface and 1.015×10^{-6} m for the lower surface. Thus the surfaces can not be considered as nominally flat, since their wave height is greater than the average valve of their maximum roughness height.

Thermometry. - The same type of thermocouple wire was used to instrument the tungsten specimen as for this one, however, the wire was butt welded at its ends. These thermocouples were calibrated in the specimen after the test was completed and were found to be within the manufacturers tolerance of ±1.1 K for the range of temperatures encountered. The couples were peened into slots milled into the circumference of the specimen. The slots were approximately 0.076 cm long, 0.033 cm wide, and at their deepest point were approximately 0.051 cm deep. The thermocouple's insulated lead wires were wrapped around the circumference of the specimen to minimize conduction errors in the thermocouple wire. Four couples were located in the upper portion of the specimen at 1.27, 2.54, 3.81, and 5.08 cm from the interface of contact. Six couples were located in the specimen's lower portion at 1.27, 2.54, 3.81, 6.35, 8.89, and 11.5 cm from the interface of contact.

Experimental Determination of h

Tungsten specimen test procedure. - The coefficient of thermal contact conductance of the tungsten - tungsten specimen was experimentally determined by using Eq. (9) and the test apparatus described above. Heat was transferred from a source, across the tungsten - tungsten interface of contact, and then to a heat sink (see fig. 6). The rate of heat transferred was determined with the aid of an OFHC heat meter. The test specimen was designed so that a one-dimensional linear heat-transfer analysis would apply. Thus the hypothetical Δt of Eq. (7) was experimentally determined by a linear extrapolation of thermal gradients from the upper and lower portions of the specimen to the interface (see fig. 5). As pointed out in Ref. 7, at the time the experiment was performed several power interruptions occurred during the test. It was found, however, that the effects caused by these interruptions could be eliminated from the analysis without introducing an error. Thus the data presented here for analysis are correct and usable. They show the cyclic variation of h versus apparent contact pressure produced during the loading and unloading of two nominally flat tungsten surfaces in a high vacuum environment. For a more detailed explanation of the tungsten test procedure see Ref. 7.

The average time needed to establish steady-state conditions after a change was made in pressure was found in Ref. 7 to be approximately $2\frac{1}{2}$ hr. After a change in interface temperature was made steady-state conditions were established in a minimum time of 3 hr, with the maximum being 45 hr. These intervals of time were considered adequate based on previous experience. However, information obtained since then indicates exposure time of about 50 hr should be allowed after a change is made in test conditions.

The interface surfaces of contact were cleaned with acetone before installation in the test facility.

Armco iron specimen test procedure. - The coefficient of thermal contact conductance of the Armco iron-Armco iron specimen was experimentally determined by using Eq. (9). The rate of heat transferred across the interface of contact was determined by calibrating the Armco iron test specimen with a 99.993 percent pure aluminum (by assay) heat meter. The contact conductance tests were performed by varying the interface contact pressure in a monotonic increasing then decreasing manner through two complete cycles from approximately 4.45×10^5 to 3.45×10^6 N/m^2 (64.5 to 500 psi) while maintaining the mean interface temperature of the test specimen nearly constant.

To gain an idea of the time required to establish equilibrium between changes in pressure and/or temperature the test specimen was exposed to steady-state test conditions for periods ranging from 50 to 180 hr between each point. Fig. 8 shows a typical variation with time of the conductance after a change from 8.0×10^5 to 10.7×10^5 N/m^2 was made in the apparent contact pressure during the first loading cycle. It will be noted that the test facility required approximately 50 hr to reach a stable condition.

Before placing the test specimen in the test column of the bell jar it was cleaned with acetone and baked out in a separate vacuum facility at 10^{-6} torr, through eight 20 min heating and cooling cycles. Each cycle varied from room temperature to approximately 450 K, well below the recrystallization temperature of Armco iron.

Data reduction. - The experimental interface temperature difference Δt (eq. (7)) was determined by the linear extrapolation of the thermocouple data to the interface of contact for both of the specimens. A simplification in this procedure was made by determining the thermal gradient in each portion of a specimen from two thermocouple readings in the same manner as that used by Fried.[4] The gradients determined by this technique were continually checked by plots including all of the thermocouple data from each specimen. The error in the temperature difference across the interface

introduced by this method was less than 1.1 K from a best line fit (drawn) through all the thermocouple data from each specimen.

Measurements of Parameters For Theoretical Determination of h

The theoretical value of h was determined from values of δ, k, and I together with Eq. (14). The quantities of δ and I were evaluated from the test specimens. The variation with temperature of the tungsten's thermal conductivity k was estimated from the literature as noted in Ref. 7. The variation of k with temperature for the Armco iron specimen was determined from calibration data obtained in the test facility under vacuum conditions from a 99.993 percent (by assay) pure aluminum heat meter. The results of this calibration indicate agreement with data from the literature[10] within $1\frac{1}{2}$ percent.

Measurement of δ. - A Brush surfanalyzer was used to determine the magnitude of δ for both specimens. It consists of a control unit, a stylus drive unit, a 50-mg stylus probe, and a recorder unit. This apparatus records the surface roughness (width and height), profile, waviness, and arithmetic average height. All of these quantities are defined in Ref. 9.

During the approach of two rough, nominally flat surfaces the maximum roughness height would make contact first. Therefore, it is appropriate to determine the average value of the maximum roughness heights δ_1 (upper) and δ_2 (lower) of the test specimen before the test is begun. Since it is not possible to obtain surface analyzer traces which include all the points of contact on a surface, a representative number of profile traces must be taken. From each of these profile traces, a single value of the maximum roughness height is obtained. These values are then averaged to obtain the value of the roughness height used in the calculations. The value of δ, where $\delta = \delta_1 + \delta_2$, is referred to as the effective value of the thermal disturbance. The values of δ_1 and δ_2 determined for the tungsten specimen were obtained by averaging the maximum roughness heights obtained from six profile traces which were made at different positions on each face of the specimen perpendicular to its ground lay. The values determined for the Armco iron specimen were obtained by averaging the maximum roughness heights obtained from ten profile traces, five taken perpendicular to the other five, on each face of the specimen.

Measurement of I. - As mentioned in Ref. 7 several authors have found that the microhardness of their specimens typically increases as the indenter load decreases. These increases have amounted to several multiples of the Meyers hardness values for these materials. The tungsten-tungsten microhardness tests reported here also indicated an increase in surface microhardness as the indenter load was decreased. The data were obtained with a Knoop indenter at room temperature and are shown in Fig. 9. The increase in the surface microhardness is attributed to surface work hardening caused by the method of preparation. The value of the microhardness, I, to be used in Eq. (14) for the tungsten specimen was taken from Fig. 9 in the light load range. These data are from the softer of the two contact surfaces.

Discussion of Results

The discussion is separated into first the presentation of the tungsten-tungsten specimen's results, and then those of the Armco Iron - Armco Iron specimen, because the test specimens are distinct and dissimilar.

Tungsten Specimen

Fig. 10 presents the Tungsten - Tungsten data from Ref. 7. During the loading portion of the cycle the data were obtained by loading the specimen's interface of contact from zero to 2.65×10^6 N/m^2 so that the surface asperities deformed plastically at a constant interface temperature of 390 K (solid square symbols in fig. 10). The interface was then loaded to 5.30×10^6 N/m^2 while its temperature was kept constant. At 5.30×10^6 N/m^2 the interface temperature was raised in three increments from 390 K to a high of 666 K (solid triangles). Finally the pressure was lowered in two steps to a low value of 4.82×10^5 N/m^2 (open symbols). At each step three changes in interface temperature were made.

The dashed curve labeled plastic theory was determined by the method presented in Ref. 7 and was calculated from Eq. (19). A second dashed curve labeled elastic theory indicates the theoretical variation of the coefficient of thermal contact conductance with apparent contact pressure during the disengagement of two nominally flat surfaces. If the interface temperature is maintained at a constant value, the theoretical prediction of this variation is dependent only on the highest apparent contact pressure that the surfaces experience. Thus agreement is indicated if the data displays the same slope as that of the theoretical variation. The symbols containing numbers in Fig. 10 indicate the sequence in which the data were obtained. They also separate the data into distinct groups which, as mentioned in Ref. 7, were bounded by power failures. Because of the likelihood that microscopic lateral asperity misalignment took place, due to large interface differential temperature effects, it is assumed that the data for each of these groups are independent of the others. The data represented by the solid symbols (plastic data) were obtained during the loading portion of the test while the open symbols indicate elastic data obtained during the unloading portion. The curves of Fig. 10 result by joining like temperature data in each of the subgroups. Separating the data in this manner has resulted in curves having slopes which agree well with plastic or elastic theory. The curve and points labeled as plastic theory show the effects of temperature. This effect appears in the theoretical representation of the coefficient of thermal contact conductance, Eq. (14), through the coefficient of thermal conductivity, k, and the surface microhardness, I. The variation with temperature of k was obtained from the literature, while that of I was obtained by the new method described in Ref. 7. The variation of I with temperature determined in this

manner was verified by experimental data from the literature. The experimental data (solid symbols) obtained during the first half of the test cycle, shown in Fig. 10 and labeled t_i = 390 K, are approximately 20 percent lower than predicted from plastic theory and calculated from Eq. (14). This agreement is considered good.

Armco Iron Specimen

Figs. 11(a) to 11(d) present data for two loading and unloading cycles obtained from the Armco Iron-Armco Iron specimen. The solid reference curves labeled elastic and plastic variation are shown for comparison with the data. The functional relationships for these curves come from Eqs. (1), (2), and (12) and the Bowden and Tabor model.[3] The data shown in Fig. 11(a) indicate that the specimen's interface surfaces of contact did not plastically deform during the loading portion of the first cycle. Thus an elastic cyclic variation would be expected to manifest itself during the remainder of the test and, indeed, it has as shown in Figs. 11(b) to 11(d). The data were obtained by initially loading the specimen's interface of contact from zero to 4.45×10^5 N/m^2 at an interface temperature of approximately 367 K. The interface was then loaded in steps to 3.45×10^6 N/m^2 while maintained at a constant temperature, thus completing the loading portion of the first cycle. The specimen was then unloaded (fig. 11(b)), reloaded (fig. 11(c)), and finally unloaded (fig. 11(d)) to complete two cycles, while the interface temperature was maintained at a constant value of approximately 367 K.

In Fig. 11(a) the dashed curve labeled theory of Clausing was determined by application of the method of Ref. 6 and was calculated from Eq. (3). The values of the constriction ratio, x_c, were determined from Eq. (4) where the contacting surfaces' radii of curvature, r_1 and r_2, were determined from surface analyzer traces of the specimen's waviness. Examples of these traces are shown in Fig. 7. The experimental data, showing the variation of h with apparent contact pressure in Fig. 11(a), are approximately 40 percent greater than predicted by the theory of Clausing. This agreement is considered good. The lack or agreement is believed due to the difficulty of determining the specimen's radii of curvature from the surface analyzer traces. As noted in comparing Figs. 11(b) to 11(d) the data display a distinct reversibility.

Comparison of Experimental Results With the Bowden and Tabor Model

Eqs. (3), (14), and (18) present the elastic or plastic theoretical variation of the coefficient of thermal contact conductance with apparent contact pressure for the specific models considered in this paper. Thus the cyclic loading and unloading of two surfaces maybe characterized as deforming according to either the elastic or plastic laws of deformation. The Bowden and Tabor model of the contact mechanism[3] describes an ideal contact composed of two surfaces irregularities which are similar to those making contact on real surfaces. The Bowden and Tabor model differs from a real surface in the number of contacting asperities. Thus a comparison of the sequence of events that take place during the cyclic contact of two real surfaces and those predicted by the Bowden and Tabor model can be helpful to an understanding of the contact phenomena. Fig. 10 shows that during the initial loading phase the conductance varies according to the plastic deformation theory of Ref. 7 as calculated from Eq. (14). During the unloading portion of the cycle the data vary according to the elastic deformation theory as calculated from Eq. (18). Thus the tungsten specimen's data indicate good agreement with the Bowden and Tabor model. The data of Fig. 11(a) for the Armco iron specimen shows that during the initial loading phase the conductance varies according to the elastic deformation theory of Refs. 5 and 6 as calculated from Eq. (3). Figs. 11(b) to 11(d) indicate reversibility which confirms the existance of elastic deformation. Therefore, the Armco iron specimen's data also show good agreement with the Bowden and Tabor model since plastic deformation of the surfaces did not occur throughout the test.

The data obtained from these two specimens not only confirms that the Bowden and Tabor model describes the contact phenomena, but they point up the necessity of varying test conditions in a specific manner so that the elasto-plastic history of events which occur during the engagement and disengagement of the surfaces may be observed. A lack of consideration of the distinction between elastic and plastic deformation phenomena and the resulting improper scheduling of an experimental test sequence has led to confusion in earlier experimental results.

Hysteresis Effects

Data presented in Ref. 4 were gathered during the initial loading, unloading and cyclic reloading of contact surfaces. These data show what experimenters frequently refers to as hysteresis effects. The data obtained here-in indicate that the so-called hysteresis effects may be caused by the unintentional use of non-steady-state data. Specifically, most experimentalists conduct their tests by attempting to establish steady-state conditions before they take their data. This is generally done by observing the emf output of the specimen's thermocouples at random points in time. Once these outputs appear to be steady over a prescribed interval of time the data are taken; thus the data are assumed to represent a steady-state condition. The experimental data presented here are the result of recording data at a prescribed test condition for times longer by an order of magnitude than previously done by many investigators. From a plot of these data versus time, an example of which is shown in Fig. 8, a steady-state average value of the coefficient of thermal contact conductance was determined for each prescribed testing condition. The resulting data for the Armco iron-Armco iron specimen (figs. 11(a) to 11(d)) indicate that no significant hysteresis effects took place. Rather small shifts in the data occurred which were caused by the inexact matching of test conditions from one point to the next. In addition, the tungsten-tungsten data (fig. 10) indicate that after loading the specimen from

2.66×10^6 to 5.31×10^6 N/m^2 predictable offsets occurred at higher contact pressures and interface temperatures.

Summary of Results

A recently published simplified approximate theoretical method for predicting the coefficient of thermal contact conductance[7] has been applied to a tungsten-tungsten specimen. The specimen's interface of contact consisted of two rough, nominally flat, outgassed surfaces in contact and under load in a high vacuum environment. Good agreement was obtained between the theory and test data. The method of calculation does not require the use of a computer for the determination of any abstract quantities; it does, however, require the use of a surface analyzer and microhardness tester. The surface analyzer provides profile traces which are used only to confirm that the specimen's surfaces of contact are nominally flat and to determine the average value of their maximum roughness heights. Thus a major simplification has been made in the computation.

Good agreement was obtained between the macroscopic elastic deformation analysis of Clausing,[6] and the thermal contact conductance test data versus apparent contact pressure obtained from two smooth non flat, outgassed Armco iron-Armco iron surfaces placed in contact and under load in a high vacuum environment. The specimen was run through two complete loading cycles and the test data showed reversible effects which were anticipated from theoretical considerations. Test data presented in this paper show that the coefficient of thermal contact conductance of two distinct and dissimilar specimens, tungsten and Armco iron, versus apparent contact pressure in the lightly load range (4.5×10^5 to 5.7×10^6 N/m^2) vary according to the sequence of elastic and plastic deformation phenomena described by the Bowden and Tabor model of contact. The test data were obtained during the cyclic loading of the two specimens. These results point up the necessity of varying test conditions in a special way so that the elasto-plastic history of events which occur during the engagement and disengagement of the surfaces may be observed.

A steady state testing procedure which exposes a specimen to long-time testing conditions has shown that the hysteresis effects, referred to in the literature, are probably caused by the use of non-steady-state test data and/or the inexact matching of test conditions from one point to the next during the performance of the test.

Symbols

A total cross-sectional area of cylindrical model, or apparent area of contact, m^2

A_c summation of individual areas of button contacts (results in total area of actual contact), m^2

A_c' contact area of one asperity, m^2

a circular contact radius, m

b radius of specimen, m

C constant

E Young's modulus of elasticity, N/m^2

h coefficient of thermal contact conductance, kW/(m^2)(K)

I microhardness, N/m^2

k coefficient of thermal conductivity, W/(m)(K)

L length of specimen's upper or lower portion, m

P total load applied to specimen divided by entire cross-sectional area (apparent contact pressure) N/m^2

P' apparent contact pressure of an asperity, N/m^2

$\dot{Q}$ rate of heat transfer, W

r radius of curvature of the surfaces in contact, m

t temperature, K

Δt extrapolated temperature difference across the interface of contact, K

Δt_c temperature difference across the effective zone of the thermal disturbance, K

W applied load acting over the total surface of contact, N

W' load applied to asperity in contact, N

W_0 upper value of loading in plastic range of softer metal (load acting over total nominally flat surface), N

W_0' upper value of asperity loading in plastic range of softer metal, N

x length from interface of button contacts along axis of cylinder, m

x_c constriction ratio or square root of the area ratio of contact, a/b

δ effective zone of the thermal disturbance or average of the maximum roughness heights of a surface, m

ν Poison's ratio

Subscripts:

c plane of button contact

i interface

0 condition of maximum loading

$1,2$ stations or offset in area of contact

References

1. Morey, T. F. and Gorman, D. N., "Thermal Design, Analysis, and Testing of a Full-Scale Planetary Lander Model," Paper 69-612, June 1969, AIAA, New York, N. Y.

2. Fletcher, L. S., Smuda, P. A., and Gyorog, D. A., "Thermal Contact Resistance of Selected Low-Conductance Interstitial Materials," AIAA Journal, Vol. 7, No. 7, July 1969, pp. 1302-1309.

3. Bowden, F. P. and Tabor, D., The Friction and Lubrication of Solids, Clarendon Press, Oxford, 1950, pp. 5-24.

4. Fried, E., "Study of Interface Thermal Contact Conductance," R66SD4471, NASA CR-82778, July 1966, General Electric Co., Philadelphia, Pa.

5. Clausing, A. M. and Chao, B. T., "Thermal Contact Resistance in a Vacuum Environment," ME-TN-242-1, 1963, University of Illinois Engineering Experiment Station, Urbana, Ill.

6. Clausing, A. M., "Heat Transfer at the Interface of Dissimilar Metals - The Influence of Thermal Strain," International Journal of Heat and Mass Transfer, Vol. 9, No. 8, Aug. 1966, pp. 791-801.

7. McKinzie, D. J., Jr., "Simplified Method for Calculating Thermal Conductance of Rough, Nominally Flat Surfaces in High Vacuum," TN D-5627, 1970, NASA, Cleveland, Ohio.

8. Fenech, H. and Rohsenow, W. M., "Prediction of Thermal Conductance of Metallic Surfaces in Contact," Journal of Heat Transfer, Vol. 85, No. 1, Feb. 1963, pp. 15-24.

9. Anon., "Surface Texture, Surface Measurement," USA Standards Institute B 46.1-1962.

10. Anon., "Thermophysical Properties Research Center Data Book, Vol. 1 - Metallic Elements and Their Alloys," 1960, Purdue University, Lafayette, Ind., Fig. 1011, Curves 2 and 12.

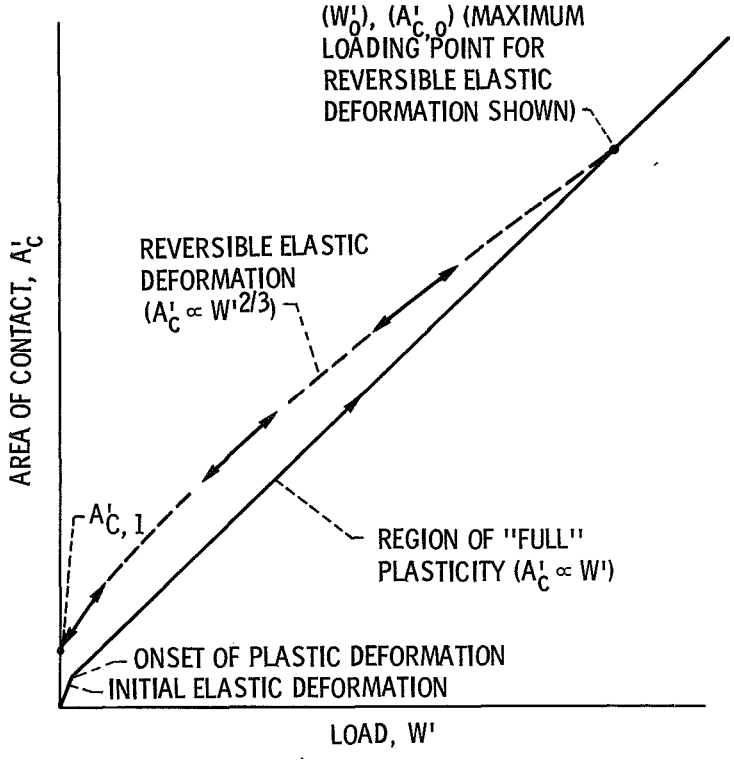

Figure 1. - Area of contact as function of load for increasing and decreasing load application to a single asperity indenting a flat plate (ref. 3).

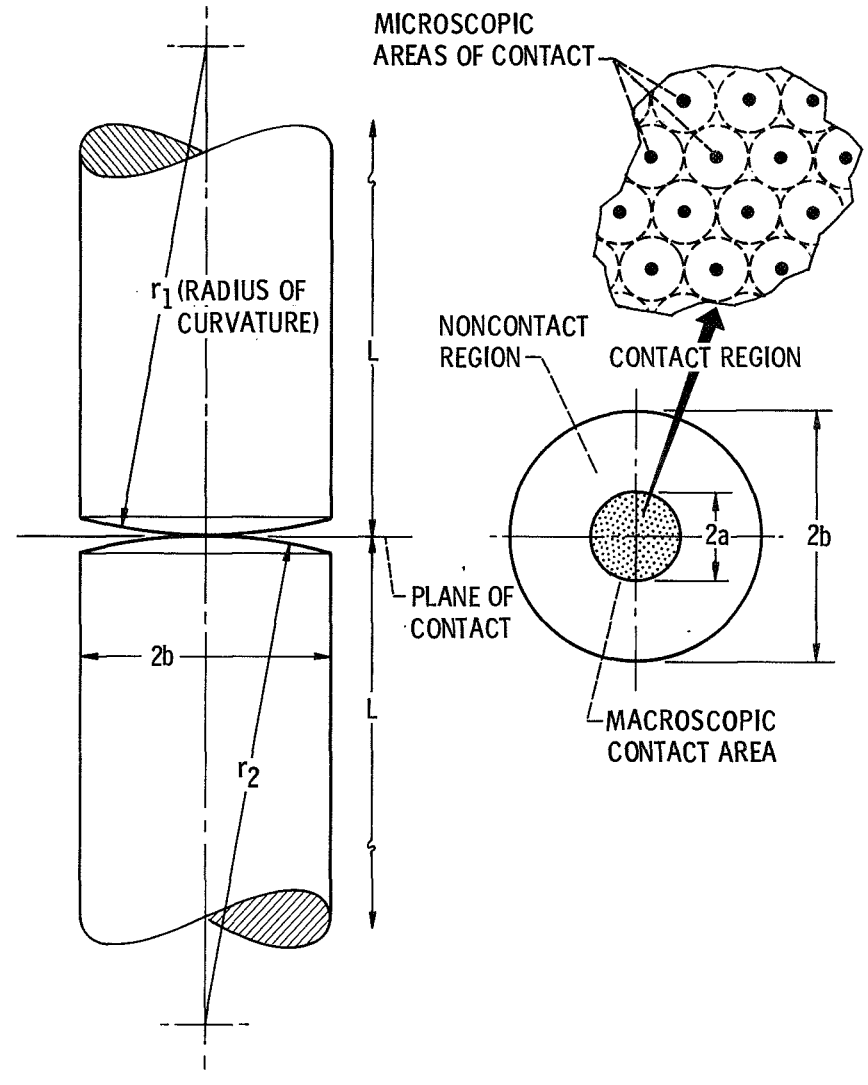

Figure 2. - Macroscopic constrictive resistance model of Clausing and Chao (ref. 5).

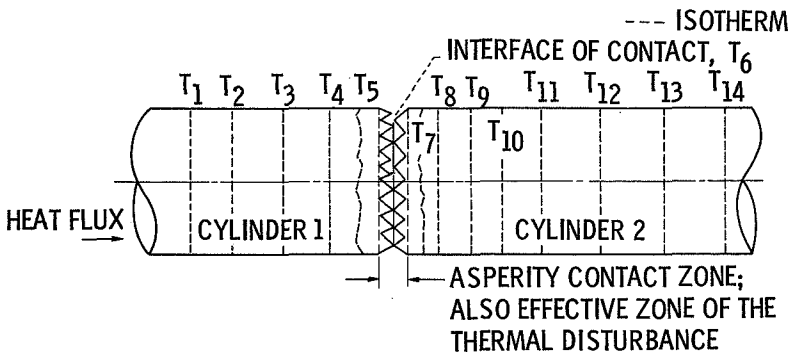

Figure 3. - View of nominally flat contact interface showing the effective zone of the thermal disturbance. $T_1 > T_{14}$.

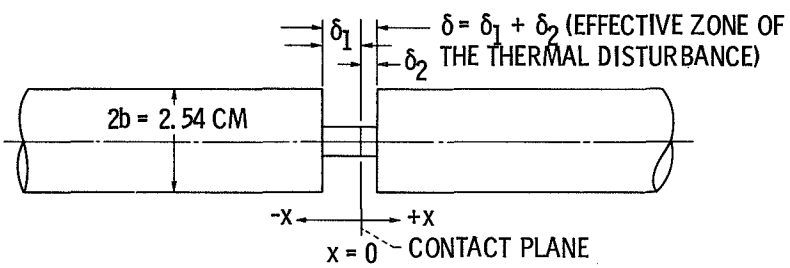

Figure 4. - Sum of areas of contact are shown in form of one button contact and the effective zone of the thermal disturbance.

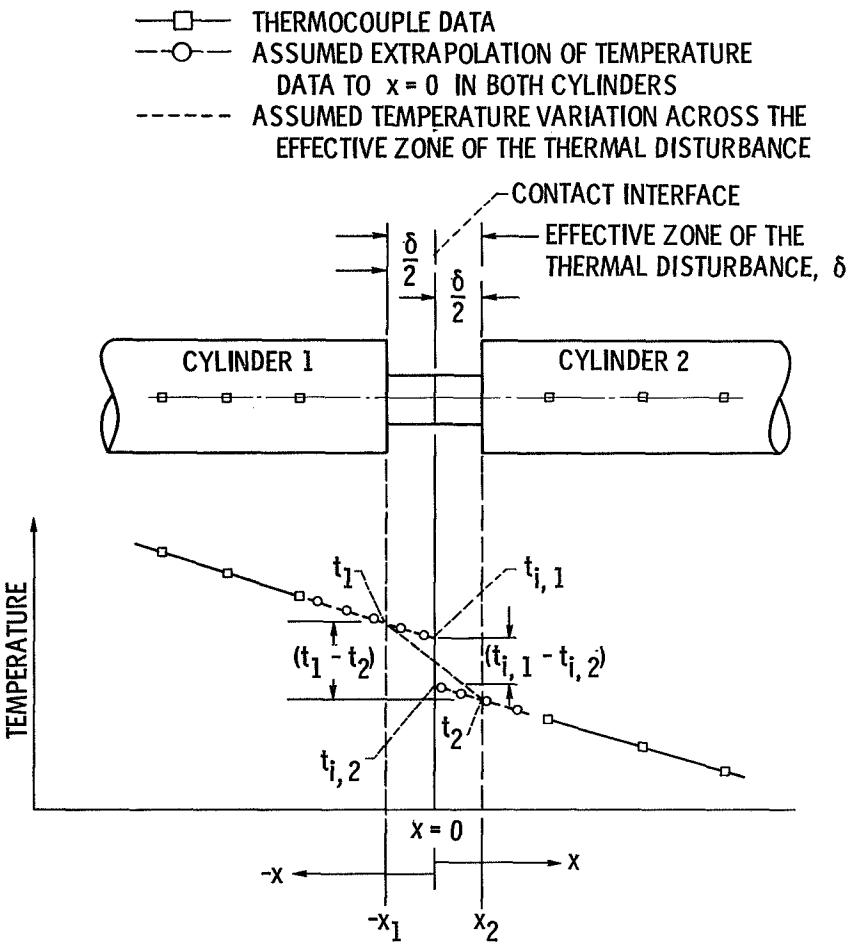

Figure 5. - Temperature profile along specimen.

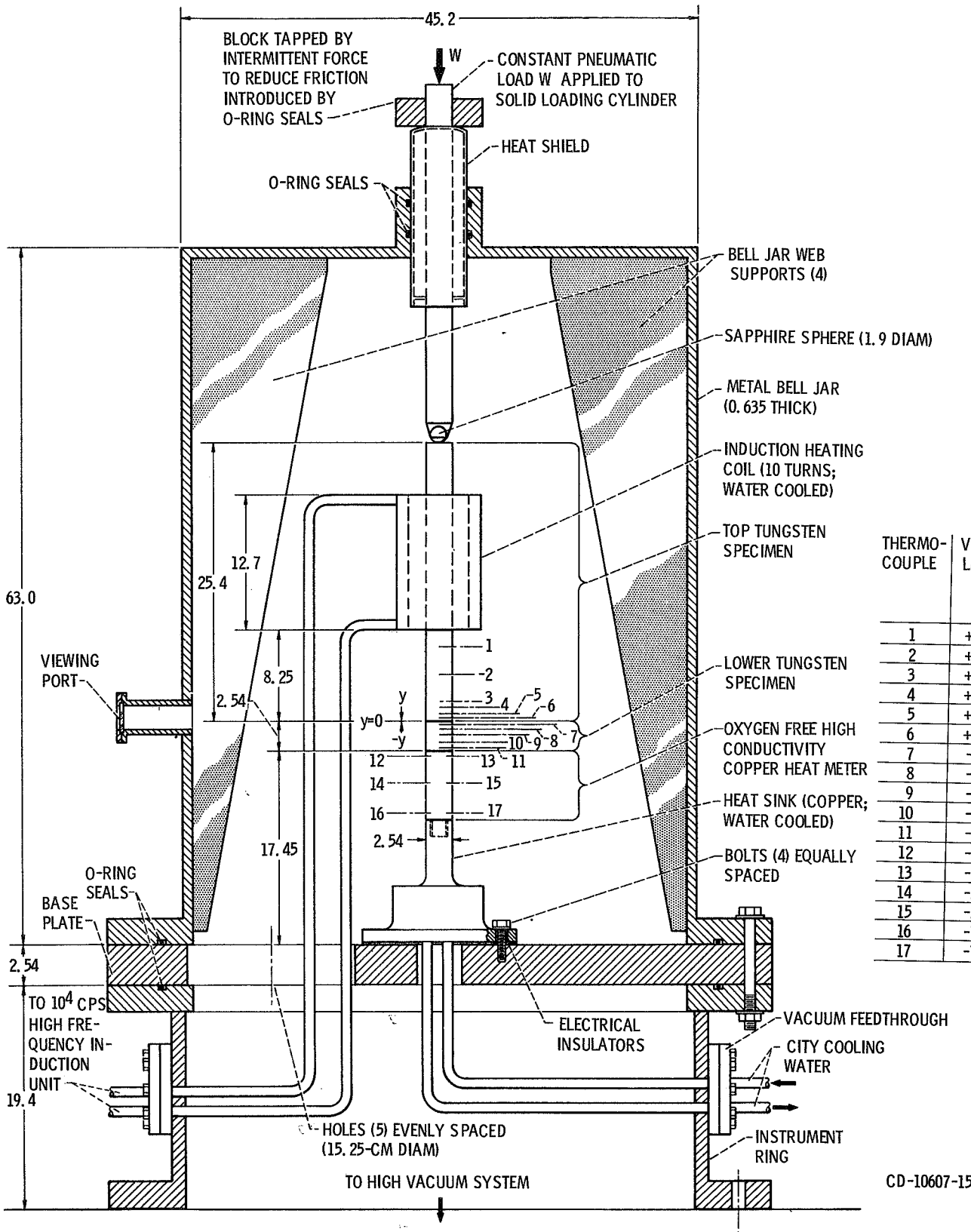

THERMOCOUPLE	VERTICAL LENGTH, y, CM
1	+6.980
2	+4.450
3	+1.905
4	+1.270
5	+0.635
6	+0.318
7	-0.318
8	-0.635
9	-0.955
10	-1.588
11	-2.222
12	-2.860
13	-2.860
14	-5.400
15	-5.400
16	-7.940
17	-7.940

Figure 6. - Internal view of bell jar. (All dimensions are in cm.)

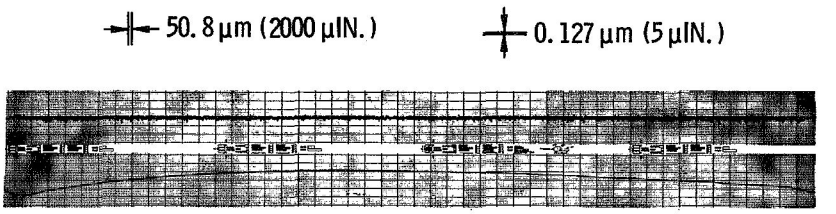

(A) ROUGHNESS ONLY (UPPER TRACE) AND WAVINESS ONLY (LOWER TRACE).

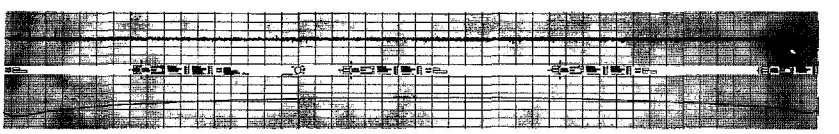

(B) ROUGHNESS ONLY (UPPER TRACE) AND WAVINESS ONLY (LOWER TRACE).

Figure 7. - Brush Surfanalyzer traces of the Armco iron specimen's top surface of contact. The tracks of the traces (a) and (b) are perpendicular to each other along diameters of the specimen's circular area of contact. Shown are typical traces of the roughness only and waviness only.

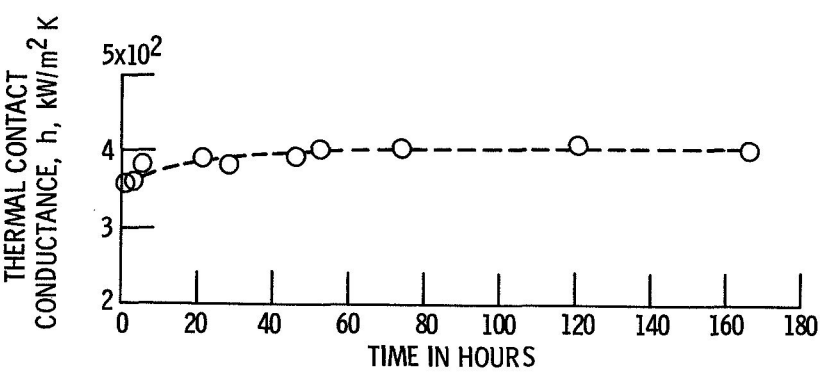

Figure 8. - Thermal contact conductance versus time for Armco Iron - Armco Iron specimen at an interface temperature of 367 K and 1.07×10^6 N/m^2.

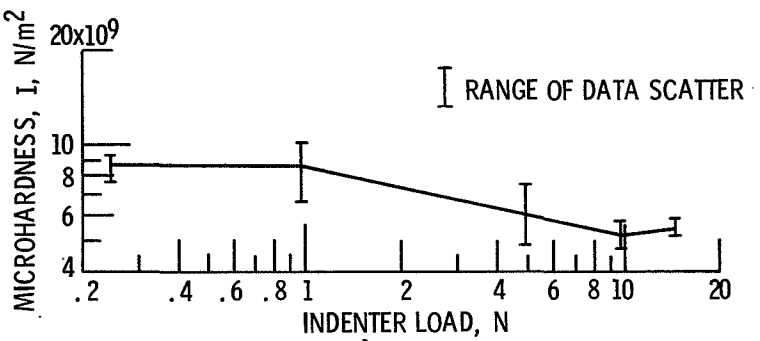

Figure 9. - Microhardness of interface surface of tungsten-tungsten specimen as function of indentor loadings at approximately 294 K.

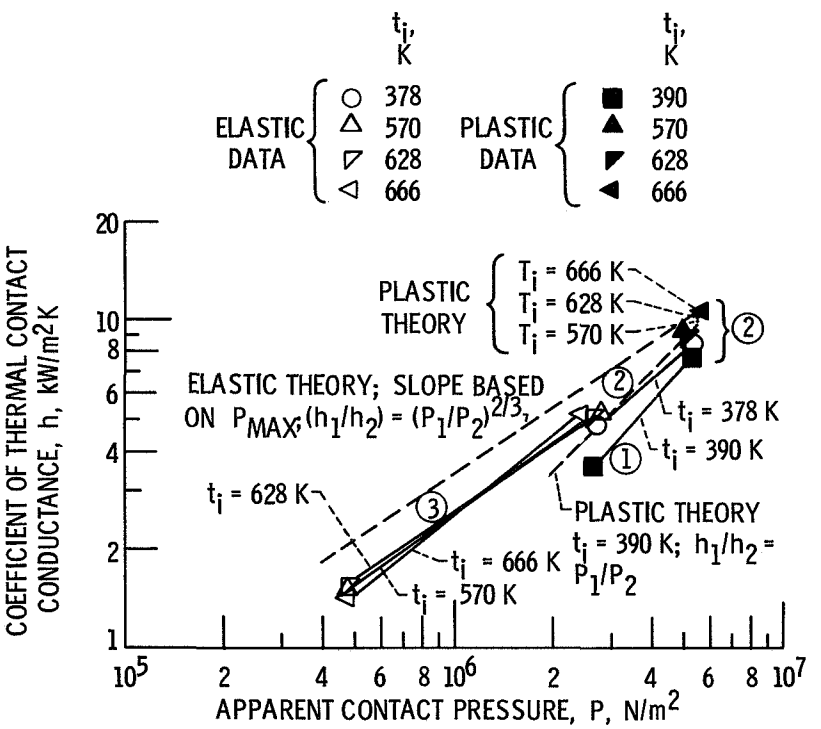

Figure 10. - Selected steady-state tungsten-tungsten data from reference 7. Lays of surfaces in contact were approximately parallel.

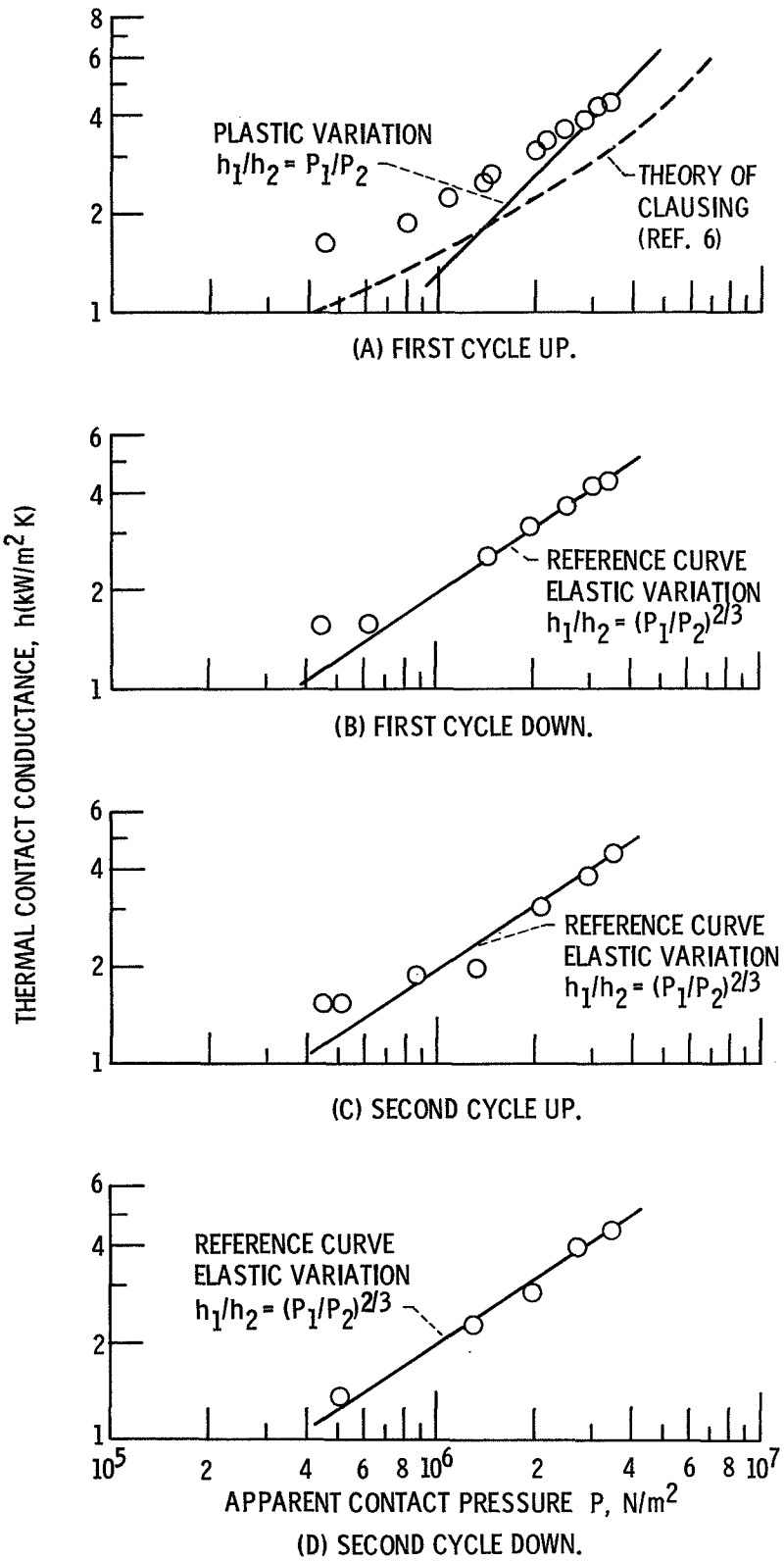

Figure 11. - Thermal contact conductance versus pressure for Armco Iron - Armco Iron. Interface temperature, $t_{I,F.}$ = 367 K: δ_1 = 0.64 μm; (crest to trough height)$_1$ = 1.30 μm. δ_2 = 0.97 μm; (crest to trough height)$_2$ = 0.58 μm.